Article

Quantifying the Chemical Composition and Real-Time Mass Loading of Nanoplastic Particles in the Atmosphere Using Aerosol Mass Spectrometry

Sining Niu, Ruizhe Liu, Qian Zhao, Sahir Gagan, Alana Dodero, Qi Ying, Xingmao Ma, Zezhen Cheng, Swarup China, Manjula Canagaratna, and Yue Zhang*

Read Online

ACCESS | 📊 Metrics & More | 📰 Article Recommendations | 🆘 Supporting Information

ABSTRACT: Plastic debris, including nanoplastic particles (NPPs), has emerged as an important global environmental issue due to its detrimental effects on human health, ecosystems, and climate. Atmospheric processes play an important role in the transportation and fate of plastic particles in the environment. In this study, a high-resolution time-of-flight aerosol mass spectrometer (HR-ToF-AMS) was employed to establish the first online approach for identification and quantification of airborne submicrometer polystyrene (PS) NPPs from laboratory-generated and ambient aerosols. The fragmentation ion $C_8H_8^+$ is identified as the major tracer ion for PS nanoplastic particles, achieving an 1-h detection limit of 4.96 ng/m^3. Ambient PS NPPs measured at an urban location in Texas are quantified to be 30 ± 20 ng/m^3 by applying the AMS data with a constrained positive matrix factorization (PMF) method using the multilinear engine (ME-2). Careful analysis of ambient data reveals that atmospheric PS NPPs were enhanced as air mass passed through a waste incinerator plant, suggesting that incineration of waste may serve as a source of ambient NPPs. The online quantification of NPPs achieved through this study can significantly improve our understanding of the source, transport, fate, and climate effects of atmospheric NPPs to mitigate this emerging global environmental issue.

KEYWORDS: *nanoplastic particles (NPPs), aerosol mass spectrometer (AMS), polystyrene (PS), positive matrix factorization (PMF), multilinear engine (ME-2), real-time measurement*
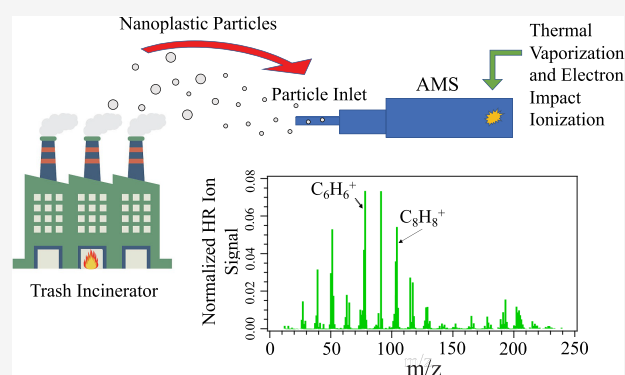
1. INTRODUCTION

Micro- and nanoplastics (MNPs), defined as plastic particles with a diameter between 1 μm and 5 mm and below 1 μm, respectively, have been an emerging environmental concern in the global ecosystem.[1−3] Microplastic particles (MPPs) were first identified as plastic debris in the environment, but subsequent studies showed that nanoplastic particles (NPPs) have distinctive physicochemical behavior and biological interactions due to their smaller sizes. Both MPPs and NPPs (herein referred to as the MNPs) can be classified as either primary or secondary plastic particles based on their sources.[4] Primary MNPs are plastic products emitted directly into the ambient environment,[5] and secondary MNPs are the decomposition fragments of larger scale plastic waste.[3] After being release into the environment, large plastic debris may undergo different transformations related to natural or anthropogenic activities, including aggregation, chemical degradation, and interaction with microorganisms,[6,7] to form MNPs. It has been shown that MNPs are emitted to the ambient environment during all stages of their lifecycle, from production to usage and waste treatment.[8] Aside from the adverse impacts of these plastic particles to the ecosystems, previous studies have also demonstrated that airborne plastic particles may also affect climate by enhancing the ice nucleation efficiency and, therefore, cloud formation.[9,10] In addition, MNPs are shown to negatively impact human health as they can enter the food chain and human body through inhalation[11] and ingestion.[12] Compounds made of plastics have already been detected in human placental tissue[13] and bloodstream[14] and can cause inflammatory reactions and oxidative stress.[15,16]

Due to the high demand for plastic materials, MNPs have been widely spreaded globally, including but not limited to the

marine environment,[17] freshwater,[18] land and soil,[19] and atmosphere.[2] Having a large volume and being the final reservoir for surface water runoffs, the marine environment has been an important sink for the MNPs.[20,21] However, studies examining the plastic cycle and plastic transportation among different environmental matrices demonstrate that atmospheric transportation also plays a crucial role in the spreading and fate of MNPs.[8,22] The atmospheric transportation of plastic materials is relatively rapid compared with other processes,[22] which facilitate the long-range movement of plastic from their sources to remote areas.[23−27]

To date, various offline chemical analysis techniques have been used to passively or actively sample and analyze atmospheric MNPs.[2] The collected samples often require additional sample preparation, including but not limited to preconcentration, organic matrix removal, and density separation.[2,28,29] The prevailing analytical methods include visual identification with microscopy,[18] thermochemical methods utilizing pyrolysis−gas chromatography−mass spectrometry (pyrolysis-GC/MS),[30] and vibrational spectroscopy using Fourier-transform infrared (FTIR) spectroscopy[31] or Raman spectroscopy,[32] all of which are offline methods that require days to weeks of sampling.[31,33] It is worth noting that even though most of the thermochemical methods requires pretreatment of the samples, a recent study shows that collected filter samples can be analyzed directly with pyrolysis-GC/MS without pretreatment due to the low matrix natural for atmospheric samples.[34] Aside from often needing pretreatments, many studies utilizing the methods described above are also constrained by the size of the plastic particles. The size limitations for analyzing plastic fragments are estimated to be 500 μm for visual methods,[35] 20 μm for FTIR,[31] and 10 μm for Raman spectroscopy, respectively.[32,36] For thermochemical methods, the traditional size limit for analyzing plastic particles was suggested to be 100 μm to obtain a clear result.[2] However, there have been significant improvements with pyrolysis-GC/MS that can identify and quantify lab-generated and ambient plastic particles with much smaller size.[34,37,38] Considering these size constraints, previous studies have focused more on microplastics with sizes ranging from 5 mm to 1 μm.[2,21] NPPs have smaller sizes, higher cell affinity, and enhanced surface curvature, making them easier to penetrate into freshwater biological barriers and accumulate in organs than MPPs.[39−42] Despite their longer atmospheric resident time, enhanced accumulation in the environment, and adverse health effects, nanoplastic particles remain largely uninvestigated due to their small sizes.[2,8,43] Hence, it is imperative to identify the chemical composition and mass concentration of nanoplastic particles to accurately assess their potential climate effects and public health risks.[44]

Herein, this study demonstrates a real-time online measurement to characterize atmospheric submicrometer polystyrene (PS) NPPs. Polystyrene is top five most abundant plastic compositions produced[2,45] and identified in the marine system.[46,47] To the best of our knowledge, this study is the first online method to measure real-time nanoplastics both in the laboratory and in the ambient environment using a high-resolution time-of-flight aerosol mass spectrometer (HR-ToF-AMS). A calibration curve was first established by sampling standard monodispersed PS particles under laboratory conditions. Our results demonstrated that the mass spectra of PS particles can be successfully separated from a complex mixture of inorganic and organic aerosol populations through

multivariate factor analysis. A tracer ion of PS NPPs, $C_8H_8^+$, was then identified by combining laboratory results with ambient measurements. Finally, the mass concentration of atmospheric PS nanoplastic particles was quantified from ambient samplings, with back trajectory analysis suggesting that trash incineration is a potential source. These results are expected to further improve our understanding of the source, evolution, and fate of atmospheric nanoplastic particles.

2. MATERIALS AND METHODS

2.1. Working Principle of the Aerosol Mass Spectrometer (AMS). The high-resolution time-of-flight aerosol mass spectrometer (HR-ToF-AMS) combines a standard vacuum mass spectrometer and aerosol sampling techniques for quantitative measurements of airborne particular matter, with detailed operation principals described in Supporting Information Section S1.[48−50] Briefly, the airborne particles are focused into a narrow beam through the aerodynamic lens at the inlet and transported into the vacuum, while the gas molecules were deflected. The particles are then directed to a tungsten vaporizer, where the nonrefractory particles are flash-vaporized upon collision. An electron impact (EI) ionizer is employed to ionize the organic molecules into ions, which are then detected by a time-of-flight mass spectrometer.[48−50] The high-resolution AMS allows direct separation of ions with the same nominal m/z, and the quantification is possible due to the reproducibility of EI ionization, similar efficiency for all nonrefractory species, and little matrix effect.[51] The HR-ToF-AMS (herein referred to as AMS) has been widely used in the atmospheric aerosol sciences,[48−51] and it was employed in all the laboratory experiments and ambient sampling of this study.

2.2. Laboratory-Generated PS Particles and Organic/Inorganic Aerosol Mixtures. To obtain the mass spectra of the pure PS NPP standards, an aqueous solution containing 500 nm monodispersed PS particles (Millipore Sigma, Part Number MFCD00243243) was aerosolized with a constant output atomizer (TSI, Model 3076). The size of 500 nm was carefully selected as this size falls within the accumulation mode, where particles typically have longer atmospheric lifetime compared with those in Aitken mode or coarse mode.[52] Given that AMS evaporates all nonrefractory submicrometer particles efficiently, 500 nm PS particle standards can represent typical NPPs and thus were used for all the lab experiments in this study. A customized silica gel diffusion dryer was used to remove the excess water prior to directing the PS particles to the AMS. The particle mass spectra were collected as a function of time.

To further characterize PS NPPs by mimicking the externally mixed particles in the ambient environment, both inorganic and secondary organic aerosols (SOAs) were generated and externally mixed with PS NPPs of selected ratios. The inorganic aerosols, including ammonium nitrate (Sigma-Aldrich, ≥98% purity) and ammonium sulfate (Sigma-Aldrich, ≥99% purity), were dissolved in Milli-Q water (mass fraction of 0.1%) and then atomized with a collision nebulizer (CH Technologies, USA). The SOAs were generated from the oxidation of selected volatile organic compound (VOC) precursors with ozone or OH radical in a potential aerosol mass (PAM) oxidation flow reactor (Aerodyne Research, Inc.).[53,54] Both biogenic (α-pinene, Sigma-Aldrich, 98% purity) and anthropogenic (toluene, Sigma-Aldrich, ≥99.5% purity) VOCs were used to generate SOA so as to obtain a more realistic scenario of nanoplastic particles mixed with
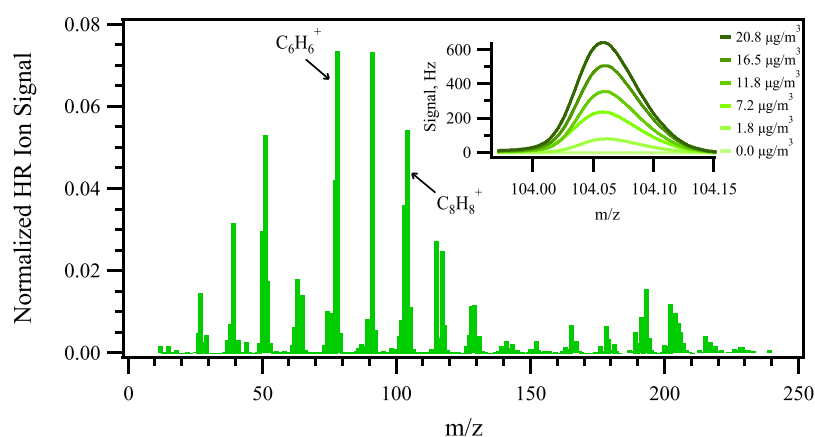
Figure 1. HR-ToF-AMS organic mass spectra for pure PS particles. Inset: the gaussian fit for tracer ion $C_8H_8^+$ under different mass concentrations of PS NPPs, which were indicated by the legend, during the calibration.

other types of aerosols in the ambient environment. The normalized number and mass distributions of the SOA measured by the scanning electrical mobility spectrometer (SEMS, Brechtel, model 2100) are shown in Figure S1. The details of PAM operations are listed in Supporting Information Section S1. Briefly, the VOC precursor was injected into a three-necked manifold at constant rate by a syringe pump (Chemyx, Model Fusion 400) and carried out by 1 L per minute (LPM) flow of zero air. The ozone was generated through an in-house customized ozone generator at a flow rate of 1.5 LPM. The reaction of the VOC with ozone in the PAM produced homogeneously nucleated SOA particles, which were then mixed with PS NPPs downstream before being analyzed by the AMS. The detailed flowchart and schematic diagram of the experimental setup are shown in Figure S2. Each reaction condition was repeated with five different mixing ratios of PS NPPs and laboratory-generated aerosols by adjusting the flow rates of two respective lines. The atomizer, sampling line, and PAM were flushed with deionized water, dry air, and ozone between experiments to prevent potential contaminations after each set of experiments. The mass spectra were collected with the AMS in *V* mode, and the data were analyzed with the Squirrel (version 1.65) and Pika (version 1.25) packages in Igor Pro (WaveMetrics Inc., version 8.04).

2.3. Ambient Sampling. To quantify the PS NPPs and their potential sources in the atmosphere, ambient particle sampling was conducted twice at the Texas A&M University, College Station, TX, which are referred to as ambient1 and ambient2 hereafter. The sampling inlet was located at the Eller Oceanography & Meteorology Building and 40 m above ground level to minimize local and surface influence. To further validate the identification and quantification of nanoplastic particles, atomized PS particles were injected intentionally into the ambient environment at a distance of 10 cm from the AMS sampling inlet toward the end of the sampling period during ambient1 and at selected times during ambient2 samplings, with detailed schematic of the setup shown in Figure S3.

2.4. Deriving Nanoplastic Mass Concentrations Using Positive Matrix Factorization (PMF) and the Multilinear Engine (ME-2). The positive matrix factorization (PMF) method was applied to the time-series mass spectral data to separate the PS particles from inorganic aerosols and SOAs. PMF is a multivariate factor analysis model that has been widely used in source apportionment of atmospheric

components.[55] Specifically, PMF has been applied to aerosol mass spectrometry for factor separation by decomposing the mass spectra and signal of the measured aerosol population with a linear combination of various factors, with detailed working principles of PMF described in Supporting Information Section S2 and brief operational procedures described below.[56−58] The isotope-excluded data and error matrices for PMF were first generated in the analysis software Pika. With a selected solution, the minimum summation of the weighted square residuals, Q, was calculated. Normalizing the Q value with the expected Q value (Q_{exp}), defined as a function of the size of the data matrix and the number of the factors, was used as a key parameter to evaluate the results.[57] The PMF analysis was performed with Igor PMF version 3.07.

To quantify the nanoplastic particles with low mass concentration from ambient atmospheric environments, the bilinear model of the multilinear engine (ME-2),[59] which allows the use of constrained factor profiles, was applied to the collected mass spectra. Compared with unconstrained PMF, ME-2 with a pre-existing input mass spectral profile will direct the bilinear model toward an optimal solution under certain situations where PMF underperforms. Generally, ME-2 is particularly suited for scenarios with factors that have similar temporal variation, relatively low concentration, and high rotational ambiguity.[60] Ambient airborne NPPs are suitable for ME-2 analysis due to their low concentration in the environment. In the ME-2 analysis, the constraint factor, namely, the *a* value, has been utilized in previous studies to define the AMS mass spectra for a specific factor.[60−62] The *a* value determines the extent to which the derived factor profile could vary from the input spectrum profile. The software package for ME-2, SoFi (Source Finder),[60] was used to identify ambient PS NPPs, and the detailed description of ME-2 is shown in Supporting Information Section S3.

3. RESULTS AND DISCUSSION

3.1. Chemical Characterization of Pure PS Nanoplastic Particles. The high-resolution mass spectrum of PS NPP was collected by the AMS, as shown in Figure 1. The mass spectrum was dominated by C_xH_y, with a ratio of 93 ± 3% by mass. As PS is made of long chains of ethenylbenzene monomers (C_8H_8), electron ionization fragments the long chains and generates C_xH_y. There were also minor fragmentation ions in the AMS mass spectra containing oxygen and nitrate (<2%), which could come from either the

oxidation of PS particles or the heated vaporizer region of the AMS. Among the C_xH_y family, $C_6H_6^+$, $C_7H_7^+$, and $C_8H_8^+$, corresponding to mass-to-charge ratios (m/z) of 78, 91, and 104 in unit mass resolution (UMR), were the three major ions in the PS mass spectrum. Given that organic species in atmospheric aerosols often fragment in the AMS to form ions with odd mass-to-charge ratios (except for nitrogen-containing compounds),[63] ions with even mass-to-charge ratios from the PS mass spectrum, such as m/z 78 and 104, are potentially unique to PS-containing particles and are further discussed in Section 3.4.

In aerosol mass spectrometry, ionization efficiency (IE), which reflects the number of ions detected per molecule sampled, is a key term in quantifying the absolute mass of the compound.[50] In addition to an IE calibration with nitrate,[49,50] an analogous calibration for PS particles was carried out with an AMS and a mixing condensation particle counter (CPC, model 1720, Brechtel). The signal of total organic concentration obtained by the AMS versus the mass concentration of PS particles derived from the CPC is shown in Figure 2,
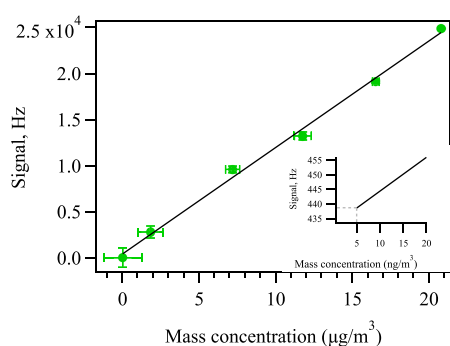
Figure 2. Calibration curve of PS particles with a slope value of 1.155 × 10^3 Hz/(μg/m^3) and R^2 = 0.995. The x-axis is the mass concentration of PS particles calculated based on the CPC measurements, and the y-axis shows the organics signal measured by the AMS. Inset: the vertical dashed line represents the detection limit calculated based on the calibration curve, while the horizonal dashed line represents the 3σ of the noise averaged over 1-h period.

demonstrating the accurate calibration of PS particles. By assuming a collection efficiency (CE) of 1, which is adopted from ammonium nitrate particles between 100 and 1000 nm,[48,64] the IE of the PS is calculated to be 1.155 × 10^3 Hz/(μg/m^3), corresponding to the slope shown in Figure 2. Based on the calibration data, the detection limits for PS particles with AMS are calculated to be 12 and 5 ng/m^3 for 10 min and 1 h of sampling, respectively, derived from three times the standard deviation of blank signals when a filter was installed at the AMS inlet.[65] Such low detection limits enable real-time quantification of ambient nanoplastic particles using the AMS. The RIE of PS particles is 1.88 with respect to nitrate assuming a unity CE, with detailed calculations and mass spectra shown in Supporting Information Section S4 and Figures S4−S7.

To further validate the quantification of PS NPPs with the AMS, a pyrolysis-GC/MS analysis was also conducted on the same samples analyzed by the AMS, with details discussed in Supporting Information Section S5 and Figure S8. Briefly, the PS NPP standards were collected by both the AMS and glass fiber filters (Cytiva, 0.7 μm particle retention) simultaneously. The mass loadings quantified by pyrolysis-GC/MS and AMS agree reasonably well within 2% of uncertainty. The above

validation further confirms accurate quantifications of PS NPPs by the AMS.

3.2. PS Factor Extracted from the Mixtures of Laboratory-Generated Aerosols. To mimic complex ambient aerosols mixed with PS nanoplastic particles, binary systems consisting of selected types of inorganic aerosols and SOAs externally mixed with PS particles in a mixing tube are analyzed by the AMS. The PS NPPs are identified and quantified using the PMF as described in Section 2. As indicated by the PMF results, more than 99% of the total mass could be well explained by the two aerosol sources (i.e., two factors) with the scaled residual (Q/Q_{exp}) dropping significantly with two factors. The diagnostic plots, including Q/Q_{exp} and scaled residual for the ammonium nitrate mixture, are shown in Figure S9 as an example. These two-source results from the PMF analysis on the mixture mass spectra are consistent with the experimental setup, where two lines of aerosols were mixed. In addition, as the ratio of the flow rates from the two aerosol sources was changed, PMF results also successfully captured the variations of the concentration of different factors, as indicated by the time series of the two factors in Figure S10.

The normalized spectra for the PS NPP factor derived from the mixture using the PMF method can reproduce the spectrum for pure PS particles with an averaged coefficient of determination R^2 = 0.95, as shown in Figure 3 and Figure
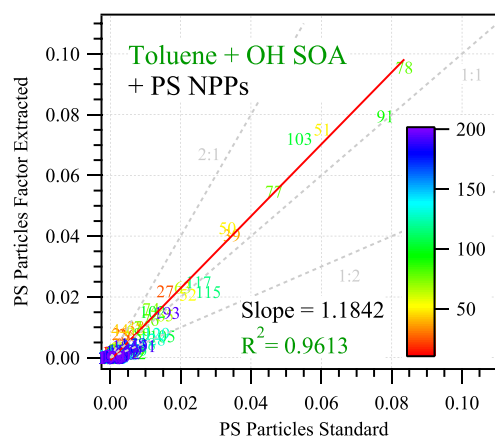
Figure 3. Scatter plot of normalized HR organic ion signal of PS particles from the factor extracted from PMF (y axis) versus the pure standard (x axis) for the binary mixture system containing toluene SOA and PS particles. The numbers are the m/z from the mass spectra. The color bar represents the values of the m/z from the mass spectrum in ascending order.

S11. The correlation slopes between the mass spectrum derived from the PMF and the mass spectrum of the PS particle standards vary between 1.06 and 1.20 depending on the composition of the mixture. Careful examination of the correlation data suggests that the mass spectra of the PS NPP factor from the organic mixtures are less dominated by m/z 104 compared with the standards. The difference of m/z 104 suggests that a small fraction of other ions from the SOAs might be partially assigned to the PS NPP factor, causing the ratio of m/z 104 to the whole mass spectra to be lower and the slopes of the correlation plots in Figure 3 and Figure S11 to be slightly higher than unity. The uncertainty for characterizing PS from a mixture of lab-generated aerosol particles with PMF is estimated to be around 20%, calculated from the deviation of
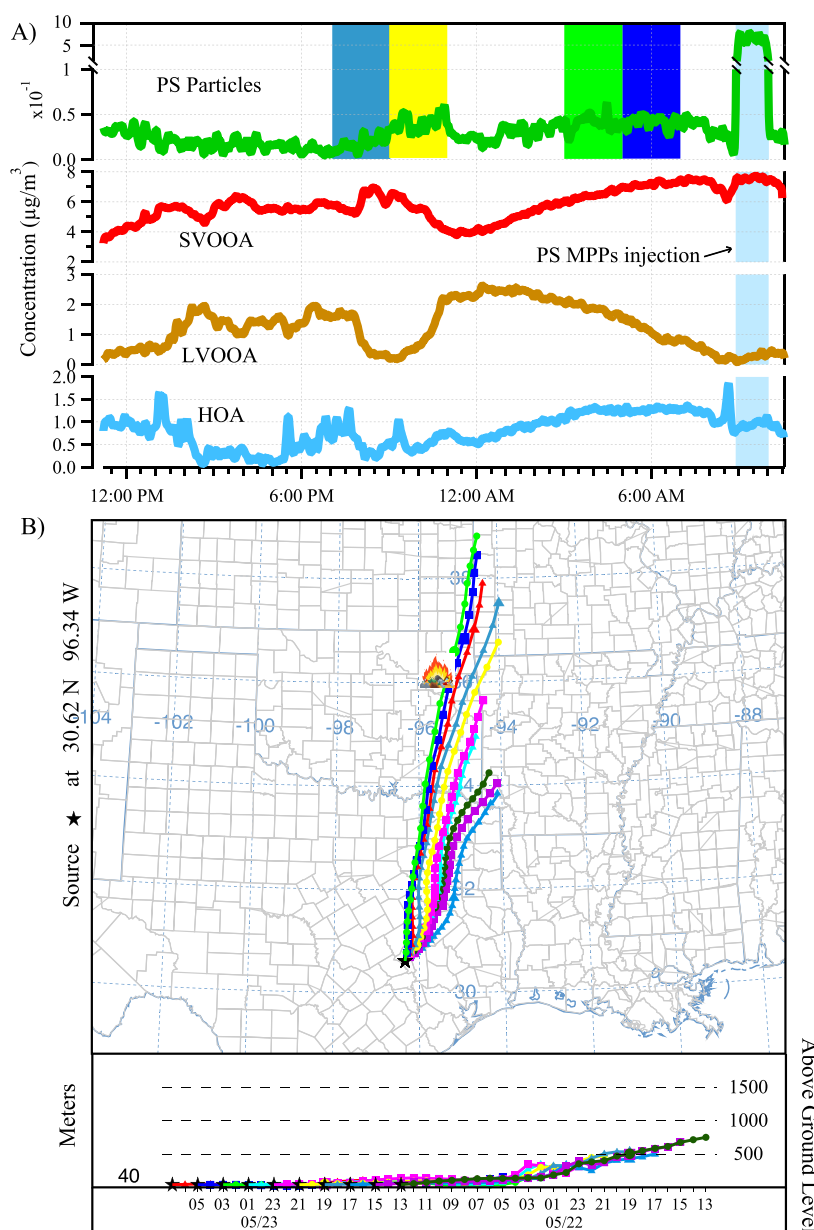
Figure 4. The time series of each factor identified during ambient1 from the ME-2 analysis (A), and the 24 h backward trajectories of air masses arriving at the sampling inlet (B) at 40 m above ground level during ambient1. The trajectories were retrieved every 2 h to elaborate the trend of derived PS factor. In Panel A, the four intervals during which the backward trajectories passed in close proximity to the waste incinerator were highlighted with the same color as their corresponding trajectories in Panel B. The legend and air mass height at the bottom of Panel B show the arrival time of the air mass at the sampling site every 2 h. These four intervals showed elevated nanoplastic concentrations.

the correlation slopes from unity as shown in Figure 3 and Figure S11. The above results successfully demonstrate that PS nanoplastic particles could be separated from common atmospheric aerosols by using the PMF factor extraction method with an uncertainty range of 20% .

3.3. Concentration of Ambient Airborne PS Nano-plastic Particles. In this study, ambient air was also sampled by an AMS to quantify the atmospheric PS NPPs. Due to the much lower concentration of PS nanoplastic particles compared with the laboratory experiments, the ME-2 method was applied to the dataset to improve the factor extraction and subsequent quantification. The ME-2 algorithm only con-strains the mass spectra of PS nanoplastic particles while allowing self-identification of other factors. The final solution was carefully chosen based on the correlation of the profiles as

well as time series information on the retrieved factors, the relative residual, and the tracer ions.[60,62]

After performing ME-2 analysis, the best ME-2 solution for the ambient1 sampling period had 4 factors, with each of the time series and mass spectra shown in Figure 4A and Figure S12, respectively. The first factor is constrained by the pure PS mass spectrum, corresponding to the PS NPPs. Two types of OOA, i.e., more-oxidized OOA (MO-OOA) and less-oxidized OOA (LO-OOA), are identified in ambient1 sampling. The factor corresponding to MO-OOA showed a higher O:C ratio and f_{44} compared with LO-OOA, agreeing with previous literature results.[66,67] Moreover, the time series of MO-OOA and LO-OOA are uncorrelated, suggesting that they may be from different air mass with different sources.[66,67] The fourth factor represents the hydrocarbon-like organic aerosol (HOA)

with the highest H:C ratio and lowest O:C ratio of all nonplastic factors. The HOA factor here also matches with those reported from previous literature with relatively higher signal intensities at m/z 55 ($C_4H_7^+$) and 57 ($C_4H_9^+$), which have been identified as markers of fresh fossil fuel combustion.[68−70] The correct assignment of plastic and other non-plastic factors further validate the ME-2 analysis results and demonstrate that ME-2 can be used for source apportionment of aerosol composition including nanoplastic particles. The diagnostic plots in Figure S13 show the scaled residual as a function of time and m/z. The 10 to 90 percentiles of the scaled residual lie between ±3, further validate support the assignment of factors from the ME-2 results.[71] The results of ambient2 are similar to those of ambient 1, with the details described in Supporting Information Section S6 and Figure S14.

As discussed in Section 2.3, PS NPPs were injected near the sampling inlet at selected periods of sampling to validate the quantification of the AMS. During the period when PS NPPs were released into the air near the sampling inlet (blue shaded area in Figure 4A), factor 1, representing the PS NPPs, was the only factor that showed a significant enhancement of its measured concentration, while the total organic concentration (Figure S14) and all other factors remained stable. The stability of other factors further validates that only factor 1 represents the concentration of ambient PS NPPs. To verify the reliability and reproducibility of the ME-2 results, two sensitivity tests were performed to determine the level of constraint to the reference profile of PS particles. For the first sensitivity test, we construct the a value of the PS NPP factor from 0.2 to 0.7, resulting in averaged concentrations of PS particles fluctuated by 16%, suggesting that the factors derived for PS nanoplastic particles are generally stable and robust despite changing a values.[60,62,72,73] For the second sensitivity test, a series of synthetic organic aerosol data containing known concentrations of PS NPPs are analyzed with ME-2. The time series of PS NPPs ranging from 16.2 to 333 ng/m^3 were synthetically added to the time series of organic aerosol mass spectra collected from ambient measurement with PS NPP profile removed. The concentrations of the PS NPP derived from this synthetic data set using the ME-2 analysis agree with the prior-known concentrations of the PS NPPs added to the spectra, as shown in Table S1. Furthermore, ME-2 analysis could successfully and accurately extract hidden PS NPP concentrations as low as 16.2 ng/m^3, a value even below the ambient concentration of PS NPPs measured from this study. Such results further validate accurate source apportionment of airborne polystyrene nanoplastic particles via online mass spectrometry coupled with the ME-2 analysis down to tens of nanograms. The detailed sensitivity analysis procedures are shown in Supporting Information Section S7.

The average concentration of PS NPPs in the ambient environment was estimated to be 30 ± 20 ng/m^3 based on the time series data of the ME-2 results and excluding the time periods when PS NPPs were artificially introduced into the air. To date, most studies that quantify atmospheric microplastics have relied on passive collection, followed by microscopic analysis. The concentration of different types of total MNPs quantified in previous studies can be estimated to ranges from 2 to 8 × 10^9 ng/m^3,[25,74−77] spanning 9 orders of magnitude regarding the mass of deposited or suspended airborne microplastics, with detailed procedures for such estimation shown in Supporting Information Section S8.[2] In general, the

more polluted the environments are, the more airborne microplastics that were identified. However, variations of concentrations among different sites occur and can be attributed to either different background environments or the size ranges targeted by each study. The wide range and large fluctuations observed from past measurements underscore the importance of an online quantitative analytical method for atmospheric nanoplastic particles. The derived concentration of PS nanoplastic particles in our sampling site is on the lower end of the estimated concentration range listed above, which is reasonable considering that our site is in a relatively clean rural area, as indicated by the low total organic aerosol concentration. Long-term monitoring of atmospheric NPPs using the AMS for a wider range of locations is desired to examine their spatial and temporal trends and to understand their impacts on the environment.

The use of an online real-time mass spectrometer can also provide accurate concentrations of atmospheric NPPs for examining the human exposure and other health effects of plastic materials. MNPs have been shown to cause neurotoxicity,[78] inflammation,[15,16] DNA damage,[78,79] alternation of gene expression,[80] etc.[81] Based on the averaged concentration of ambient airborne NPPs derived in this study and an inhalation rate of 11 m^3/day,[82] the exposure of an adult to PS NPPs in College Station derived from this measurement is estimated to be at the order of 100 mg/year. This extrapolated annual concentration of PS NPPs assumes that the conditions are the same for indoor and outdoor environments regardless of seasonal change and thus may provide a rough estimation of potential atmospheric nanoplastic exposure that may be useful in its magnitude. In addition, the exposure calculated may skew toward the lower end due to the finding that higher concentrations of airborne microplastics were found to be present in the indoor environment than the outdoor environment.[83,84] The in vivo inhalation toxicity of PS NPPs was evaluated using a whole-body inhalation system with rats as the experimental animal.[85] Under different PS NPP exposures ranging from 22 to 100 μg/m^3 for 14 days, serum biochemistry, pulmonary function, bronchoalveolar lavage, lung tissue, and Western blot analyses of the rats were performed. The results suggested that PS NPP exposure has a distinct effect at the molecular level by increasing the inflammatory protein expression, and there exists the potential health risk at a higher level (e.g., organismal level) if the exposure is sustained.[85] Future studies are needed to examine the long-term exposure of atmospheric NPPs at ambient levels. The toxicity and concentration of PS NPPs above highlight the critical need for further research aimed at quantifying the toxicity of atmospheric nanoplastic particles with regard to their potential impacts on human health.

Other than the source apportionment bilinear model ME-2, the Hybrid Single Particle Lagrangian Integrated Trajectory model (HYSPLIT) was also applied to the stationary ambient sampling to assess the atmospheric trajectory and potential source of the PS NPPs.[86] The 24 h back trajectories of the air mass at the sampling inlet were evaluated with a 2 h time interval, and they are shown in Figure 4B. In general, during the 20 h sampling period, the measured air mass was consistently from the north of the College Station, with the altitude gradually decreasing from 800 m above ground level to 40 m at the sampling site. As indicated by the illustration in Figure 4B, a trash incineration site is located near the back trajectory pathways, and it is the only municipal waste

combustor in the surrounding area with 420 miles radius from all of the back trajectories. A careful analysis of the back trajectories of the air mass shows that when the wind direction is the closest to the trash incineration site, i.e., May 22, 8 to 11 pm, and May 23, 3 to 8 am, the ambient PS NPP concentration was elevated as indicated by the color-coded time period in Figure 4A. A t test was performed for the PS NPP data set, and the concentration during the color-coded time period in Figure 4A shows a statistically significant increase in comparison with that from 4 to 6 pm ($p < 0.01$), with detailed results shown in Table S2. Micro- and nanoplastic particles have been reported to generate from incineration with the Raman spectroscopy method,[87−89] agreeing with our ambient observation. Previous studies also have shown that nanoplastic particles comprised of both PS and polyethylene terephthalate (PET) can be generated at temperatures as low as 200 °C through homogeneous nucleation when the plastic is melted and cooled.[90,91] A waste incinerator can often be heated to 650 to 1100 °C, higher than the melting and vapor recondensation onset temperature of 200 °C from which nanoplastics can be generated. In addition, potential incomplete combustion in the incineration of waste further facilitates the generation of byproducts including nanoplastic particles.[92−95] It is worth noting that the PS NPP concentration decreased significantly between 10 pm to 2 am from March 22−23, suggesting that the PS NPP enhancement intervals before and after this period were not due to the change of the boundary layer height but likely due to external sources of PS NPPs. Other than polystyrene, as many as nine types of airborne NPPs have been reported to be generated from the flying ashes of the trash incinerators.[94,95] The above correlation between the PS NPP concentration and the passing of air mass through the trash incineration site indicates that the city's solid waste treatment could be a potential source of atmospheric NPPs.
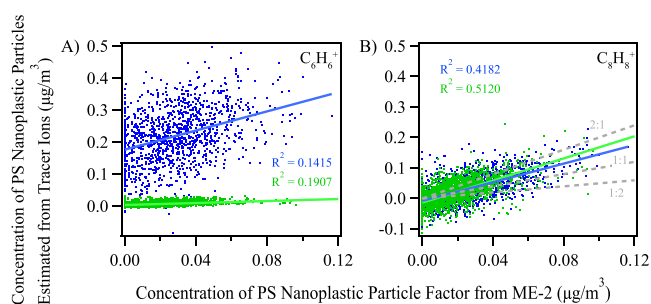
3.4. Tracer Ion of PS Nanoplastic Particles.

In Section 3.1, $C_6H_6^+$ and $C_8H_8^+$ were identified as potential tracer ions for PS NPPs from pure nanoplastic spectra and laboratory experiments with externally mixed aerosol particles. With ambient data, we further examined the robustness of these two ions serving as tracers for the PS nanoplastic particles. Figure 5 shows the correlations between the concentrations of $C_6H_6^+$ and $C_8H_8^+$ and the PS NPP factor during both ambient sampling periods. The concentrations of PS nanoplastic particles were not correlated to the signals of $C_6H_6^+$ ($R^2 = 0.14$ and 0.19 for two sampling periods) but correlated relatively well with the signals of $C_8H_8^+$ ($R^2 = 0.42$ and 0.51 for

two sampling periods). In addition, the slopes of the $C_8H_8^+$ signals from two independent field data sets are similar despite two different air mass dominating during these two sampling periods, suggesting that $C_8H_8^+$ could be a robust tracer ion. In addition, the $C_6H_6^+$ ion can also come from secondary organic aerosols, such as decomposing aromatics,[96−98] further suggesting that $C_8H_8^+$ is a better tracer for identifying PS nanoplastic compounds. It has been reported in previous studies that chitin, a natural biopolymer in water and soil that is likely from crustaceans, insects, and invertebrate animals, can release $C_8H_8^+$ during pyrolysis.[99−101] Hence, water and soil samples with complicated environmental matrices encompassing components from the biosphere may cause chitin to contribute to the $C_8H_8^+$ signal, leading to inaccurate estimation of PS NPPs with $C_8H_8^+$. However, atmospheric nanoplastic samples are generally low matrices and have less interference from the biosphere, leading to the potentially minimal influences of chitin on the quantification of NPPs.

To examine the feasibility of using tracer ion $C_8H_8^+$ to identify PS NPPs, the concentrations of PS particles are calculated from both the ME-2 analysis and tracer ion $C_8H_8^+$ with eq S4. The fraction of $C_8H_8^+$ in the mass spectrum of pure PS standards was combined with the actual signal of $C_8H_8^+$ from ambient aerosols to calculate the concentration of atmospheric PS NPPs, with details illustrated in Section S9. The concentration derived from the $C_8H_8^+$ tracer ion is 25% higher on average than the value derived from the ME-2 method. The results suggest that $C_8H_8^+$ might overestimate the ambient PS nanoplastic concentration due to other sources of $C_8H_8^+$ from the aerosols, as stated above. Given that $C_8H_8^+$ is a reduced alkane fragment, it has not been recognized as a tracer ion for the most common factors extracted by the PMF for ambient aerosols in previous studies[69,70] and has only been identified in two studies where it was attributed to monoterpene emission[102] and aromatics.[103] Other than polystyrene, there exist other types of plastic polymers in ambient NPPs, for instance, polypropylene, polyethylene, and polyvinyl chloride. Due to different chemical structures, their mass spectra from pyrolysis-GC/MS are different.[104] Hence, it is unlikely for other types of NPPs to cause large uncertainties in quantification of PS NPPs as they will likely not generate the same tracer ions of $C_8H_8^+$ as PS. Overall, given a lack of techniques in quantifying atmospheric NPPs, tracer ion $C_8H_8^+$ is still useful in identifying PS NPPs especially when statistic tools such as ME-2 are not available.

3.5. Environmental Implications and Applications.

This study establishes a real-time online method to quantify PS NPPs for the first time using an aerosol mass spectrometer and identifies the fragmentation ion $C_8H_8^+$ (m/z 104) as a potentially tracer ion for identifying and quantifying PS NPPs. The calibration curve of PS NPPs using AMS shows that this online method can achieve low detection limits of 12 and 5 ng/m³ over the course of 10 min and 1 h, respectively. Laboratory-generated binary mixtures of inorganic and organic aerosols were successfully separated from the PS NPPs using the PMF technique, with the PMF factor of PS particle successfully identified from the externally mixed aerosol population. The spectra of the PS nanoplastic factor are highly similar to those of the authentic PS standards, with $R^2 > 0.95$, suggesting that the nanoplastic mass spectra are different from those of SOA particles. Subsequent ambient measurements also derived a PS NPP factor using ME-2 analysis, with the ambient concentration of PS NPP estimated to be 30 ± 20 ng/

Figure 5. The correlation between the concentration of PS nanoplastic particle derived from tracer ions A) $C_6H_6^+$, B) $C_8H_8^+$ (y axis) and ME-2 (x axis) for ambient sampling (blue: *ambient1*, green: *ambient2*).

m^3. The annual exposure of ambient PS NPP may cause non-negligible and potentially adverse effects on human health. Back trajectory analysis demonstrates that trash incineration may also be a potentially important source of atmospheric NPPs.

For ambient data analysis, ME-2 constrains the whole mass spectrum and thus can successfully identify PS NPPs from a complex atmospheric particle population. The combination of AMS with ME-2 also has the potential to identify and quantify other types of airborne NPPs, as various types of plastics may fragment differently due to their unique molecular composition and structures.[104] Further studies are needed to verify the feasibility of identifying other types of NPPs using the AMS and to examine the health effects when exposed to ambient levels of nanoplastic particles. In summary, this real-time quantification of ambient nanoplastic particles provides a unique tool to examine the abundance, distribution, life cycle, and health and climate impacts of atmospheric nanoplastic particles, bridging the gap in understanding the role of atmosphere processes in the environmental cycle of micro- and nanoplastic particles.

ASSOCIATED CONTENT

Supporting Information

The Supporting Information is available free of charge at https://pubs.acs.org/doi/10.1021/acs.est.3c10286.

> Section S1: aerosol mass spectrometry and potential aerosol mass reactor operation conditions; Section S2: positive matrix factorization (PMF) working principle; Section S3: detailed analysis procedures of ME-2; Section S4: relative ionization efficiency (RIE) of polystyrene nanoplastic particles; Section S5: comparison of PS NPP quantification with the AMS and pyrolysis-GC/MS; Section S6: second ambient sampling; Section S7: ME-2 analysis of the synthetic data matrix; Section S8: concentration of MNPs from the literature; Section S9: concentration of PS NPPs derived from tracer ions; Figure S1: number and mass distribution of self-nucleated SOAs generated though PAM; Figure S2: schematic of the experimental setup for the mixing of PS nanoplastic particles and inorganic/organic aerosols; Figure S3: schematic of the ambient sampling setup; Figure S4: correlation heat map of the mass spectra of PS NPPs under different concentrations; Figure S5: mass spectrum of ammonium nitrate collected by the AMS during calibration; Figure S6: mass spectrum collected by the AMS with a filter at the inlet; Figure S7: derived concentration of the tracer ions of PS NPPs with a filter at the inlet of the AMS; Figure S8: mass spectrum of PS NPPs from pyrolysis-GC/MS; Figure S9: scaled residual and Q/Q_{exp} from PMF for lab experiment; Figure S10: time series of the factors extracted from the binary mixture system; Figure S11: correlation between the mass spectrum for the authentic PS particle standard and the factors extracted by the PMF; Figure S12: mass spectrum of each factor from ME-2 during ambient sampling; Figure S13: scaled residual for ambient sampling; Figure S14: time series of total organics during ambient sampling; Table S1: sensitivity analysis of ME-2 applied on ambient-level concentrations of PS NPPs; Table S2: averaged mass concentration of PS NPPs from ambient measurements and the *p*-value for *t* test (PDF)

AUTHOR INFORMATION

Corresponding Author

Yue Zhang — *Department of Atmospheric Sciences, Texas A&M University, College Station, Texas 77843, United States;* ○ orcid.org/0000-0001-7234-9672; Phone: +1 (979) 862-4401; Email: yuezhang@tamu.edu; Fax: +1(979) 862-4466

Authors

Sining Niu — *Department of Atmospheric Sciences, Texas A&M University, College Station, Texas 77843, United States;* ○ orcid.org/0000-0002-3389-0076

Ruizhe Liu — *Department of Atmospheric Sciences, Texas A&M University, College Station, Texas 77843, United States;* Present Address: Present address: School of Earth and Atmospheric Sciences, Georgia Institute of Technology, Atlanta, Georgia 30332, United States (R.L.)

Qian Zhao — *Environmental Molecular Sciences Laboratory, Pacific Northwest National Laboratory, Richland, Washington 99354, United States;* ○ orcid.org/0000-0003-4489-3691

Sahir Gagan — *Department of Atmospheric Sciences, Texas A&M University, College Station, Texas 77843, United States*

Alana Dodero — *Department of Atmospheric Sciences, Texas A&M University, College Station, Texas 77843, United States*

Qi Ying — *Department of Civil and Environmental Engineering, Texas A&M University, College Station, Texas 77843, United States;* ○ orcid.org/0000-0002-4560-433X

Xingmao Ma — *Department of Civil and Environmental Engineering, Texas A&M University, College Station, Texas 77843, United States*

Zezhen Cheng — *Environmental Molecular Sciences Laboratory, Pacific Northwest National Laboratory, Richland, Washington 99354, United States;* ○ orcid.org/0000-0001-6320-4519

Swarup China — *Environmental Molecular Sciences Laboratory, Pacific Northwest National Laboratory, Richland, Washington 99354, United States;* ○ orcid.org/0000-0001-7670-335X

Manjula Canagaratna — *Aerodyne Research Inc., Billerica, Massachusetts 01821, United States*

Complete contact information is available at:
https://pubs.acs.org/10.1021/acs.est.3c10286

Notes

The authors declare no competing financial interest.

■ REFERENCES

(1) Rochman, C. M.; Brookson, C.; Bikker, J.; Djuric, N.; Earn, A.; Bucci, K.; Athey, S.; Huntington, A.; McIlwraith, H.; Munno, K.; De Frond, H.; Kolomijeca, A.; Erdle, L.; Grbic, J.; Bayoumi, M.; Borrelle, S. B.; Wu, T. N.; Santoro, S.; Werbowski, L. M.; Zhu, X.; Giles, R. K.; Hamilton, B. M.; Thaysen, C.; Kaura, A.; Klasios, N.; Ead, L.; Kim, J.; Sherlock, C.; Ho, A.; Hung, C. Rethinking microplastics as a diverse contaminant suite. *Environ. Toxicol. Chem.* 2019, 38 (4), 703−711.

(2) Zhang, Y. L.; Kang, S. C.; Allen, S.; Allen, D.; Gao, T. G.; Sillanpaa, M. Atmospheric microplastics: A review on current status and perspectives. *Earth Sci. Rev.* 2020, 203, No. 103118.

(3) Hartmann, N. B.; Huffer, T.; Thompson, R. C.; Hassellov, M.; Verschoor, A.; Daugaard, A. E.; Rist, S.; Karlsson, T.; Brennholt, N.; Cole, M.; Herrling, M. P.; Hess, M. C.; Ivleva, N. P.; Lusher, A. L.; Wagner, M. Are We Speaking the Same Language? Recommendations for a Definition and Categorization Framework for Plastic Debris. *Environ. Sci. Technol.* 2019, 53 (3), 1039−1047.

(4) Li, W. C.; Tse, H. F.; Fok, L. Plastic waste in the marine environment: A review of sources, occurrence and effects. *Sci. Total Environ.* 2016, 566, 333−349.

(5) Dris, R.; Gasperi, J.; Saad, M.; Mirande, C.; Tassin, B. Synthetic fibers in atmospheric fallout: A source of microplastics in the environment? *Mar. Pollut. Bull.* 2016, 104 (1−2), 290−293.

(6) Zhang, K.; Su, J.; Xiong, X.; Wu, X.; Wu, C. X.; Liu, J. T. Microplastic pollution of lakeshore sediments from remote lakes in Tibet plateau, China. *Environ. Pollut.* 2016, 219, 450−455.

(7) Lowry, G. V.; Gregory, K. B.; Apte, S. C.; Lead, J. R. Transformations of Nanomaterials in the Environment. *Environ. Sci. Technol.* 2012, 46 (13), 6893−6899.

(8) Bank, M. S.; Hansson, S. V. The Plastic Cycle: A Novel and Holistic Paradigm for the Anthropocene. *Environ. Sci. Technol.* 2019, 53 (13), 7177−7179.

(9) Ganguly, M.; Ariya, P. A. Ice Nucleation of Model Nanoplastics and Microplastics: A Novel Synthetic Protocol and the Influence of Particle Capping at Diverse Atmospheric Environments. *Earth Space Chem.* 2019, 3 (9), 1729−1739.

(10) Lebedev, A. T.; Polyakova, O. V.; Mazur, D. M.; Artaev, V. B.; Canet, I.; Lallement, A.; Vaïtilingom, M.; Deguillaume, L.; Delort, A. M. Detection of semi-volatile compounds in cloud waters by GC × GC-TOF-MS. Evidence of phenols and phthalates as priority pollutants. *Environ. Pollut.* 2018, 241, 616−625.

(11) Amato-Lourenço, L. F.; Galvão, L. D. S.; De Weger, L. A.; Hiemstra, P. S.; Vijver, M. G.; Mauad, T. An emerging class of air pollutants: Potential effects of microplastics to respiratory human health? *Sci. Total Environ.* 2020, 749, No. 141676.

(12) Lwanga, E. H.; Vega, J. M.; Ku Quej, V.; Chi, J. D. l. A.; Del Cid, L. S.; Chi, C.; Segura, G. E.; Gertsen, H.; Salánki, T.; van der Ploeg, M.; Koelmans, A. A.; Geissen, V. Field evidence for transfer of plastic debris along a terrestrial food chain. *Sci. Rep.* 2017, 7 (1), 14071.

(13) Ragusa, A.; Svelato, A.; Santacroce, C.; Catalano, P.; Notarstefano, V.; Carnevali, O.; Papa, F.; Rongioletti, M. C. A.; Baiocco, F.; Draghi, S.; D'Amore, E.; Rinaldo, D.; Matta, M.; Giorgini, E. Plasticenta: First evidence of microplastics in human placenta. *Environ. Int.* 2021, 146, No. 106274.

(14) Leslie, H. A.; van Velzen, M. J. M.; Brandsma, S. H.; Vethaak, A. D.; Garcia-Vallejo, J. J.; Lamoree, M. H. Discovery and quantification of plastic particle pollution in human blood. *Environ. Int.* 2022, 163, No. 107199.

(15) von Moos, N.; Burkhardt-Holm, P.; Köhler, A. Uptake and Effects of Microplastics on Cells and Tissue of the Blue Mussel Mytilus edulis L. after an Experimental Exposure. *Environ. Sci. Technol.* 2012, 46 (20), 11327−11335.

(16) Espinosa, C.; Cuesta, A.; Esteban, M. Á. Effects of dietary polyvinylchloride microparticles on general health, immune status and expression of several genes related to stress in gilthead seabream (Sparus aurata L.). *Fish Shellfish Immunol* 2017, 68, 251−259.

(17) Peng, L. C.; Fu, D. D.; Qi, H. Y.; Lan, C. Q.; Yu, H. M.; Ge, C. J. Micro- and nano-plastics in marine environment: Source, distribution and threats - A review. *Sci. Total Environ.* 2020, 698, No. 134254.

(18) Dris, R.; Gasperi, J.; Rocher, V.; Saad, M.; Renault, N.; Tassin, B. Microplastic contamination in an urban area: a case study in Greater Paris. *Environ. Chem.* 2015, 12 (5), 592−599.

(19) Carr, S. A.; Liu, J.; Tesoro, A. G. Transport and fate of microplastic particles in wastewater treatment plants. *Water Res.* 2016, 91, 174−182.

(20) Andrady, A. L. The plastic in microplastics: A review. *Mar. Pollut. Bull.* 2017, 119 (1), 12−22.

(21) Auta, H. S.; Emenike, C. U.; Fauziah, S. H. Distribution and importance of microplastics in the marine environment: A review of the sources, fate, effects, and potential solutions. *Environ. Int.* 2017, 102, 165−176.

(22) Horton, A. A.; Dixon, S. J. Microplastics: An introduction to environmental transport processes. *Wires Water* 2018, 5 (2), e1268.

(23) Allen, D.; Allen, S.; Abbasi, S.; Baker, A.; Bergmann, M.; Brahney, J.; Butler, T.; Duce, R. A.; Eckhardt, S.; Evangeliou, N.; Jickells, T.; Kanakidou, M.; Kershaw, P.; Laj, P.; Levermore, J.; Li, D. J.; Liss, P.; Liu, K.; Mahowald, N.; Masque, P.; Materic, D.; Mayes, A. G.; McGinnity, P.; Osvath, I.; Prather, K. A.; Prospero, J. M.; Revell, L. E.; Sander, S. G.; Shim, W. J.; Slade, J.; Stein, A.; Tarasova, O.; Wright, S. Microplastics and nanoplastics in the marine-atmosphere environment. *Nat. Rev. Earth Env* 2022, 3 (6), 393−405.

(24) Ambrosini, R.; Azzoni, R. S.; Pittino, F.; Diolaiuti, G.; Franzetti, A.; Parolini, M. First evidence of microplastic contamination in the supraglacial debris of an alpine glacier. *Environ. Pollut.* 2019, 253, 297−301.

(25) Liu, K.; Wang, X.; Fang, T.; Xu, P.; Zhu, L.; Li, D. Source and potential risk assessment of suspended atmospheric microplastics in Shanghai. *Sci. Total Environ.* 2019, 675, 462−471.

(26) Zhang, Y.; Gao, T.; Kang, S.; Sillanpää, M. Importance of atmospheric transport for microplastics deposited in remote areas. *Environ. Pollut.* 2019, 254, 112953.

(27) Klein, M.; Fischer, E. K. Microplastic abundance in atmospheric deposition within the Metropolitan area of Hamburg, Germany. *Sci. Total Environ.* 2019, 685, 96−103.

(28) Shao, L.; Li, Y.; Jones, T.; Santosh, M.; Liu, P.; Zhang, M.; Xu, L.; Li, W.; Lu, J.; Yang, C.-X.; Zhang, D.; Feng, X.; BéruBé, K. Airborne microplastics: A review of current perspectives and environmental implications. *J. Clean Prod* 2022, 347, No. 131048.

(29) Wang, Y.; Huang, J.; Zhu, F.; Zhou, S. Airborne Microplastics: A Review on the Occurrence, Migration and Risks to Humans. *Bull. Environ. Contam. Toxicol.* 2021, 107 (4), 657−664.

(30) Fries, E.; Dekiff, J. H.; Willmeyer, J.; Nuelle, M. T.; Ebert, M.; Remy, D. Identification of polymer types and additives in marine microplastic particles using pyrolysis-GC/MS and scanning electron microscopy. *Environ. Sci-Proc. Imp* 2013, 15 (10), 1949−1956.

(31) Kappler, A.; Fischer, D.; Oberbeckmann, S.; Schernewski, G.; Labrenz, M.; Eichhorn, K. J.; Voit, B. Analysis of environmental microplastics by vibrational microspectroscopy: FTIR, Raman or both? *Anal Bioanal Chem.* 2016, 408 (29), 8377−8391.

(32) Allen, S.; Allen, D.; Phoenix, V. R.; Le Roux, G.; Jiménez, P. D.; Simonneau, A.; Binet, S.; Galop, D. Atmospheric transport and deposition of microplastics in a remote mountain catchment. *Nat. Geosci.* 2019, 12 (5), 339−344.

(33) Gillibert, R.; Balakrishnan, G.; Deshoules, Q.; Tardivel, M.; Magazzù, A.; Donato, M. G.; Maragò, O. M.; de La Chapelle, M. L.; Colas, F.; Lagarde, F.; Gucciardi, P. G. Raman Tweezers for Small Microplastics and Nanoplastics Identification in Seawater. *Environ. Sci. Technol.* 2019, 53 (15), 9003−9013.

(34) Sheng, X.-y.; Lai, Y.-j.; Yu, S.-j.; Li, Q.-c.; Zhou, Q.-x.; Liu, J.-f. Quantitation of Atmospheric Suspended Polystyrene Nanoplastics by Active Sampling Prior to Pyrolysis−Gas Chromatography−Mass Spectrometry. *Environ. Sci. Technol.* **2023**, *57* (29), 10754−10762.

(35) Löder, M. G. J.; Gerdts, G. Methodology Used for the Detection and Identification of Microplastics-A Critical Appraisal. In *Marine Anthropogenic Litter*, Bergmann, M.; Gutow, L.; Klages, M., Eds.; Springer International Publishing, 2015; pp 201−227.

(36) Araujo, C. F.; Nolasco, M. M.; Ribeiro, A. M. P.; Ribeiro-Claro, P. J. A. Identification of microplastics using Raman spectroscopy: Latest developments and future prospects. *Water Res.* **2018**, *142*, 426−440.

(37) Käppler, A.; Fischer, M.; Scholz-Böttcher, B. M.; Oberbeckmann, S.; Labrenz, M.; Fischer, D.; Eichhorn, K.-J.; Voit, B. Comparison of μ-ATR-FTIR spectroscopy and py-GCMS as identification tools for microplastic particles and fibers isolated from river sediments. *Anal Bioanal Chem.* **2018**, *410* (21), 5313−5327.

(38) Materić, D.; Ludewig, E.; Xu, K.; Röckmann, T.; Holzinger, R. Brief communication: Analysis of organic matter in surface snow by PTR-MS − implications for dry deposition dynamics in the Alps. *Cryosphere* **2019**, *13* (1), 297−307.

(39) Zhang, B.; Chao, J.; Chen, L.; Liu, L.; Yang, X.; Wang, Q. Research progress of nanoplastics in freshwater. *Sci. Total Environ.* **2021**, *757*, No. 143791.

(40) Li, Z.; Feng, C.; Wu, Y.; Guo, X. Impacts of nanoplastics on bivalve: Fluorescence tracing of organ accumulation, oxidative stress and damage. *J. Hazard Mater.* **2020**, *392*, No. 122418.

(41) Kolandhasamy, P.; Su, L.; Li, J.; Qu, X.; Jabeen, K.; Shi, H. Adherence of microplastics to soft tissue of mussels: A novel way to uptake microplastics beyond ingestion. *Sci. Total Environ.* **2018**, *610−611*, 635−640.

(42) Au, S. Y.; Lee, C. M.; Weinstein, J. E.; van den Hurk, P.; Klaine, S. J. Trophic transfer of microplastics in aquatic ecosystems: Identifying critical research needs. *Integr Environ. Assess Manag* **2017**, *13* (3), 505−509.

(43) Alimi, O. S.; Farner Budarz, J.; Hernandez, L. M.; Tufenkji, N. Microplastics and Nanoplastics in Aquatic Environments: Aggregation, Deposition, and Enhanced Contaminant Transport. *Environ. Sci. Technol.* **2018**, *52* (4), 1704−1724.

(44) Bhat, M. A.; Gedik, K.; Gaga, E. O. Atmospheric micro (nano) plastics: future growing concerns for human health. *Air Qual Atmos Health* **2023**, *16* (2), 233−262.

(45) PlasticsEurope, E. P. R. O. *Plastics—the facts 2019. An analysis of European plastics production, demand and waste data.* PlasticsEurope **2019**, 1 42.

(46) De Haan, W. P.; Sanchez-Vidal, A.; Canals, M. Floating microplastics and aggregate formation in the Western Mediterranean Sea. *Mar. Pollut. Bull.* **2019**, *140*, 523−535.

(47) Jones, J. I.; Vdovchenko, A.; Cooling, D.; Murphy, J. F.; Arnold, A.; Pretty, J. L.; Spencer, K. L.; Markus, A. A.; Vethaak, A. D.; Resmini, M. Systematic Analysis of the Relative Abundance of Polymers Occurring as Microplastics in Freshwaters and Estuaries. *Int. J. Environ. Res. Public Health* **2020**, *17*, 9304 DOI: 10.3390/ijerph17249304.

(48) Jayne, J. T.; Leard, D. C.; Zhang, X.; Davidovits, P.; Smith, K. A.; Kolb, C. E.; Worsnop, D. R. Development of an Aerosol Mass Spectrometer for Size and Composition Analysis of Submicron Particles. *Aerosol Sci. Technol.* **2000**, *33* (1−2), 49−70.

(49) Jimenez, J. L.; Jayne, J. T.; Shi, Q.; Kolb, C. E.; Worsnop, D. R.; Yourshaw, I.; Seinfeld, J. H.; Flagan, R. C.; Zhang, X.; Smith, K. A.; Morris, J. W.; Davidovits, P. Ambient aerosol sampling using the Aerodyne Aerosol Mass Spectrometer. *J. Geophys. Res. Atmos.* **2003**, *108* (D7), 8425.

(50) Canagaratna, M. R.; Jayne, J. T.; Jimenez, J. L.; Allan, J. D.; Alfarra, M. R.; Zhang, Q.; Onasch, T. B.; Drewnick, F.; Coe, H.; Middlebrook, A.; Delia, A.; Williams, L. R.; Trimborn, A. M.; Northway, M. J.; DeCarlo, P. F.; Kolb, C. E.; Davidovits, P.; Worsnop, D. R. Chemical and microphysical characterization of ambient aerosols with the aerodyne aerosol mass spectrometer. *Mass Spectrom Rev.* **2007**, *26* (2), 185−222.

(51) DeCarlo, P. F.; Kimmel, J. R.; Trimborn, A.; Northway, M. J.; Jayne, J. T.; Aiken, A. C.; Gonin, M.; Fuhrer, K.; Horvath, T.; Docherty, K. S.; Worsnop, D. R.; Jimenez, J. L. Field-Deployable, High-Resolution, Time-of-Flight Aerosol Mass Spectrometer. *Anal. Chem.* **2006**, *78* (24), 8281−8289.

(52) Seinfeld, J. H.; Pandis, S. N. *Atmospheric chemistry and physics: from air pollution to climate change*; John Wiley & Sons Incorporated, 2016, 325−361.

(53) Kang, E.; Root, M. J.; Toohey, D. W.; Brune, W. H. Introducing the concept of Potential Aerosol Mass (PAM). *Atmos Chem. Phys.* **2007**, *7* (22), 5727−5744.

(54) Lambe, A. T.; Ahern, A. T.; Williams, L. R.; Slowik, J. G.; Wong, J. P. S.; Abbatt, J. P. D.; Brune, W. H.; Ng, N. L.; Wright, J. P.; Croasdale, D. R.; Worsnop, D. R.; Davidovits, P.; Onasch, T. B. Characterization of aerosol photooxidation flow reactors: heterogeneous oxidation, secondary organic aerosol formation and cloud condensation nuclei activity measurements. *Atmos Meas Tech* **2011**, *4* (3), 445−461.

(55) Zhang, Q.; Jimenez, J. L.; Canagaratna, M. R.; Ulbrich, I. M.; Ng, N. L.; Worsnop, D. R.; Sun, Y. L. Understanding atmospheric organic aerosols via factor analysis of aerosol mass spectrometry: a review. *Anal Bioanal Chem.* **2011**, *401* (10), 3045−3067.

(56) Lanz, V. A.; Alfarra, M. R.; Baltensperger, U.; Buchmann, B.; Hueglin, C.; Prevot, A. S. H. Source apportionment of submicron organic aerosols at an urban site by factor analytical modelling of aerosol mass spectra. *Atmos Chem. Phys.* **2007**, *7* (6), 1503−1522.

(57) Ulbrich, I. M.; Canagaratna, M. R.; Cubison, M. J.; Zhang, Q.; Ng, N. L.; Aiken, A. C.; Jimenez, J. L. Three-dimensional factorization of size-resolved organic aerosol mass spectra from Mexico City. *Atmos Meas Tech* **2012**, *5* (1), 195−224.

(58) Slowik, J. G.; Vlasenko, A.; McGuire, M.; Evans, G. J.; Abbatt, J. P. D. Simultaneous factor analysis of organic particle and gas mass spectra: AMS and PTR-MS measurements at an urban site. *Atmos Chem. Phys.* **2010**, *10* (4), 1969−1988.

(59) Paatero, P. The Multilinear Engine—A Table-Driven, Least Squares Program for Solving Multilinear Problems, Including the n-Way Parallel Factor Analysis Model. *J. Comput. Graphical Stat.* **1999**, *8* (4), 854−888.

(60) Canonaco, F.; Crippa, M.; Slowik, J. G.; Baltensperger, U.; Prevot, A. S. H. SoFi, an IGOR-based interface for the efficient use of the generalized multilinear engine (ME-2) for the source apportionment: ME-2 application to aerosol mass spectrometer data. *Atmos Meas Tech* **2013**, *6* (12), 3649−3661.

(61) Lanz, V. A.; Alfarra, M. R.; Baltensperger, U.; Buchmann, B.; Hueglin, C.; Szidat, S.; Wehrli, M. N.; Wacker, L.; Weimer, S.; Caseiro, A.; Puxbaum, H.; Prevot, A. S. H. Source Attribution of Submicron Organic Aerosols during Wintertime Inversions by Advanced Factor Analysis of Aerosol Mass Spectra. *Environ. Sci. Technol.* **2008**, *42* (1), 214−220.

(62) Crippa, M.; Canonaco, F.; Lanz, V. A.; Äijälä, M.; Allan, J. D.; Carbone, S.; Capes, G.; Ceburnis, D.; Dall'Osto, M.; Day, D. A.; DeCarlo, P. F.; Ehn, M.; Eriksson, A.; Freney, E.; Hildebrandt Ruiz, L.; Hillamo, R.; Jimenez, J. L.; Junninen, H.; Kiendler-Scharr, A.; Kortelainen, A. M.; Kulmala, M.; Laaksonen, A.; Mensah, A. A.; Mohr, C.; Nemitz, E.; O'Dowd, C.; Ovadnevaite, J.; Pandis, S. N.; Petäjä, T.; Poulain, L.; Saarikoski, S.; Sellegri, K.; Swietlicki, E.; Tiitta, P.; Worsnop, D. R.; Baltensperger, U.; Prévôt, A. S. H. Organic aerosol components derived from 25 AMS data sets across Europe using a consistent ME-2 based source apportionment approach. *Atmos Chem. Phys.* **2014**, *14* (12), 6159−6176.

(63) Sareen, N.; Carlton, A. G.; Surratt, J. D.; Gold, A.; Lee, B.; Lopez-Hilfiker, F. D.; Mohr, C.; Thornton, J. A.; Zhang, Z. F.; Lim, Y. B.; Turpin, B. J. Identifying precursors and aqueous organic aerosol formation pathways during the SOAS campaign. *Atmos Chem. Phys.* **2016**, *16* (22), 14409−14420.

(64) Williams, L. R.; Gonzalez, L. A.; Peck, J.; Trimborn, D.; McInnis, J.; Farrar, M. R.; Moore, K. D.; Jayne, J. T.; Robinson, W. A.;

Lewis, D. K.; Onasch, T. B.; Canagaratna, M. R.; Trimborn, A.; Timko, M. T.; Magoon, G.; Deng, R.; Tang, D.; de la Rosa Blanco, E.; Prévôt, A. S. H.; Smith, K. A.; Worsnop, D. R. Characterization of an aerodynamic lens for transmitting particles greater than 1 micrometer in diameter into the Aerodyne aerosol mass spectrometer. *Atmos. Meas. Technol.* **2013**, *6* (11), 3271−3280.

(65) Drewnick, F.; Hings, S. S.; Alfarra, M. R.; Prevot, A. S. H.; Borrmann, S. Aerosol quantification with the Aerodyne Aerosol Mass Spectrometer: detection limits and ionizer background effects. *Atmos Meas Tech* **2009**, *2* (1), 33−46.

(66) Setyan, A.; Zhang, Q.; Merkel, M.; Knighton, W. B.; Sun, Y.; Song, C.; Shilling, J. E.; Onasch, T. B.; Herndon, S. C.; Worsnop, D. R.; Fast, J. D.; Zaveri, R. A.; Berg, L. K.; Wiedensohler, A.; Flowers, B. A.; Dubey, M. K.; Subramanian, R. Characterization of submicron particles influenced by mixed biogenic and anthropogenic emissions using high-resolution aerosol mass spectrometry: results from CARES. *Atmos Chem. Phys.* **2012**, *12* (17), 8131−8156.

(67) Hu, W.; Day, D. A.; Campuzano-Jost, P.; Nault, B. A.; Park, T.; Lee, T.; Croteau, P.; Canagaratna, M. R.; Jayne, J. T.; Worsnop, D. R.; Jimenez, J. L. Evaluation of the New Capture Vaporizer for Aerosol Mass Spectrometers (AMS): Elemental Composition and Source Apportionment of Organic Aerosols (OA). *Earth Space Chem.* **2018**, *2* (4), 410−421.

(68) Docherty, K. S.; Aiken, A. C.; Huffman, J. A.; Ulbrich, I. M.; DeCarlo, P. F.; Sueper, D.; Worsnop, D. R.; Snyder, D. C.; Peltier, R. E.; Weber, R. J.; Grover, B. D.; Eatough, D. J.; Williams, B. J.; Goldstein, A. H.; Ziemann, P. J.; Jimenez, J. L. The 2005 Study of Organic Aerosols at Riverside (SOAR-1): instrumental intercomparisons and fine particle composition. *Atmos Chem. Phys.* **2011**, *11* (23), 12387−12420.

(69) Zhang, Q.; Alfarra, M. R.; Worsnop, D. R.; Allan, J. D.; Coe, H.; Canagaratna, M. R.; Jimenez, J. L. Deconvolution and quantification of hydrocarbon-like and oxygenated organic aerosols based on aerosol mass spectrometry. *Environ. Sci. Technol.* **2005**, *39* (13), 4938−4952.

(70) Shah, R. U.; Robinson, E. S.; Gu, P.; Robinson, A. L.; Apte, J. S.; Presto, A. A. High-spatial-resolution mapping and source apportionment of aerosol composition in Oakland, California, using mobile aerosol mass spectrometry. *Atmos Chem. Phys.* **2018**, *18* (22), 16325−16344.

(71) Paatero, P.; Hopke, P. K. Discarding or downweighting high-noise variables in factor analytic models. *Anal. Chim. Acta* **2003**, *490* (1), 277−289.

(72) Elser, M.; Huang, R. J.; Wolf, R.; Slowik, J. G.; Wang, Q.; Canonaco, F.; Li, G.; Bozzetti, C.; Daellenbach, K. R.; Huang, Y.; Zhang, R.; Li, Z.; Cao, J.; Baltensperger, U.; El-Haddad, I.; Prévôt, A. S. H. New insights into PM$_{2.5}$ chemical composition and sources in two major cities in China during extreme haze events using aerosol mass spectrometry. *Atmos Chem. Phys.* **2016**, *16* (5), 3207−3225.

(73) Canonaco, F.; Tobler, A.; Chen, G.; Sosedova, Y.; Slowik, J. G.; Bozzetti, C.; Daellenbach, K. R.; El Haddad, I.; Crippa, M.; Huang, R. J.; Furger, M.; Baltensperger, U.; Prévôt, A. S. H. A new method for long-term source apportionment with time-dependent factor profiles and uncertainty assessment using SoFi Pro: application to 1 year of organic aerosol data. *Atmos Meas Tech* **2021**, *14* (2), 923−943.

(74) Asrin, N. R. N.; Dipareza, A. Microplastics in ambient air (case study: Urip Sumoharjo street and Mayjend Sungkono street of Surabaya City, Indonesia). *J. Adv. Res. Appl. Sci.* **2019**, *6*, 54−57.

(75) Dehghani, S.; Moore, F.; Akhbarizadeh, R. Microplastic pollution in deposited urban dust, Tehran metropolis. *Iran. Environ. Sci. Pollut Res* **2017**, *24* (25), 20360−20371.

(76) Liu, C.; Li, J.; Zhang, Y.; Wang, L.; Deng, J.; Gao, Y.; Yu, L.; Zhang, J.; Sun, H. Widespread distribution of PET and PC microplastics in dust in urban China and their estimated human exposure. *Environ. Int.* **2019**, *128*, 116−124.

(77) Liu, K.; Wu, T.; Wang, X.; Song, Z.; Zong, C.; Wei, N.; Li, D. Consistent Transport of Terrestrial Microplastics to the Ocean through Atmosphere. *Environ. Sci. Technol.* **2019**, *53* (18), 10612−10619.

(78) Ribeiro, F.; Garcia, A. R.; Pereira, B. P.; Fonseca, M.; Mestre, N. C.; Fonseca, T. G.; Ilharco, L. M.; Bebianno, M. J. Microplastics effects in Scrobicularia plana. *Mar. Pollut. Bull.* **2017**, *122* (1), 379−391.

(79) Besseling, E.; Redondo-Hasselerharm, P.; Foekema, E. M.; Koelmans, A. A. Quantifying ecological risks of aquatic micro- and nanoplastic. *Crit Rev. Environ. Sci. Technol.* **2019**, *49* (1), 32−80.

(80) Mazurais, D.; Ernande, B.; Quazuguel, P.; Severe, A.; Huelvan, C.; Madec, L.; Mouchel, O.; Soudant, P.; Robbens, J.; Huvet, A.; Zambonino-Infante, J. Evaluation of the impact of polyethylene microbeads ingestion in European sea bass (Dicentrarchus labrax) larvae. *Mar Environ. Res.* **2015**, *112*, 78−85.

(81) Koelmans, A. A.; Redondo-Hasselerharm, P. E.; Nor, N. H. M.; de Ruijter, V. N.; Mintenig, S. M.; Kooi, M. Risk assessment of microplastic particles. *Nat. Rev. Mater.* **2022**, *7* (2), 138−152.

(82) Brochu, P.; Ducré-Robitaille, J.-F.; Brodeur, J. Physiological Daily Inhalation Rates for Free-Living Individuals Aged 1 Month to 96 Years, Using Data from Doubly Labeled Water Measurements: A Proposal for Air Quality Criteria, Standard Calculations and Health Risk Assessment. *Hum Ecol Risk Assess* **2006**, *12* (4), 675−701.

(83) Dris, R.; Gasperi, J.; Mirande, C.; Mandin, C.; Guerrouache, M.; Langlois, V.; Tassin, B. A first overview of textile fibers, including microplastics, in indoor and outdoor environments. *Environ. Pollut.* **2017**, *221*, 453−458.

(84) Prata, J. C. Airborne microplastics: Consequences to human health? *Environ. Pollut.* **2018**, *234*, 115−126.

(85) Lim, D.; Jeong, J.; Song, K. S.; Sung, J. H.; Oh, S. M.; Choi, J. Inhalation toxicity of polystyrene micro(nano)plastics using modified OECD TG 412. *Chemosphere* **2021**, *262*, No. 128330.

(86) Rolph, G.; Stein, A.; Stunder, B. Real-time Environmental Applications and Display sYstem: READY. *Environ. Model Softw* **2017**, *95*, 210−228.

(87) Luo, Y.; Naidu, R.; Zhang, X.; Fang, C. Microplastics and nanoplastics released from a PPE mask under a simulated bushfire condition. *Journal of Hazardous Materials* **2022**, *439*, No. 129621.

(88) DeLoid, G. M.; Cao, X.; Coreas, R.; Bitounis, D.; Singh, D.; Zhong, W.; Demokritou, P. Incineration-Generated Polyethylene Micro-Nanoplastics Increase Triglyceride Lipolysis and Absorption in an In Vitro Small Intestinal Epithelium Model. *Environ. Sci. Technol.* **2022**, *56* (17), 12288−12297.

(89) Luo, Y.; Gibson, C. T.; Chuah, C.; Tang, Y.; Ruan, Y.; Naidu, R.; Fang, C. Fire releases micro- and nanoplastics: Raman imaging on burned disposable gloves. *Environ. Pollut.* **2022**, *312*, No. 120073.

(90) Morales, A. C.; Tomlin, J. M.; West, C. P.; Rivera-Adorno, F. A.; Peterson, B. N.; Sharpe, S. A. L.; Noh, Y.; Sendesi, S. M. T.; Boor, B. E.; Howarter, J. A.; Moffet, R. C.; China, S.; O'Callahan, B. T.; El-Khoury, P. Z.; Whelton, A. J.; Laskin, A. Atmospheric emission of nanoplastics from sewer pipe repairs. *Nat. Nanotechnol* **2022**, *17* (11), 1171−1177.

(91) Wlasits, P. J.; Konrat, R.; Winkler, P. M. Heterogeneous Nucleation of Supersaturated Water Vapor onto Sub-10 nm Nanoplastic Particles. *Environ. Sci. Technol.* **2023**, *57* (4), 1584−1591.

(92) Hintze, P. E.; Caraccio, A.; Anthony, S. M.; DeVor, R.; Captain, J. G.; Tsoras, A.; Nur, M. Trash-to-Gas: Using Waste Products to Minimize Logistical Mass During Long Duration Space Missions. In *AIAA SPACE 2013 Conference and Exposition* **2013**, 5326 DOI: DOI: 10.2514/6.2013-5326.

(93) Verma, R.; Vinoda, K. S.; Papireddy, M.; Gowda, A. N. S. Toxic Pollutants from Plastic Waste- A Review. *Procedia Environmental Sciences* **2016**, *35*, 701−708.

(94) Shen, M.; Hu, T.; Huang, W.; Song, B.; Qin, M.; Yi, H.; Zeng, G.; Zhang, Y. Can incineration completely eliminate plastic wastes? An investigation of microplastics and heavy metals in the bottom ash and fly ash from an incineration plant. *Science of The Total Environment* **2021**, *779*, No. 146528.

(95) Yang, Z.; Lü, F.; Zhang, H.; Wang, W.; Shao, L.; Ye, J.; He, P. Is incineration the terminator of plastics and microplastics? *Journal of Hazardous Materials* **2021**, *401*, No. 123429.

(96) Loza, C. L.; Chhabra, P. S.; Yee, L. D.; Craven, J. S.; Flagan, R. C.; Seinfeld, J. H. Chemical aging of m-xylene secondary organic aerosol: laboratory chamber study. *Atmos Chem. Phys.* **2012**, *12* (1), 151−167.

(97) Craven, J. S.; Yee, L. D.; Ng, N. L.; Canagaratna, M. R.; Loza, C. L.; Schilling, K. A.; Yatavelli, R. L. N.; Thornton, J. A.; Ziemann, P. J.; Flagan, R. C.; Seinfeld, J. H. Analysis of secondary organic aerosol formation and aging using positive matrix factorization of high-resolution aerosol mass spectra: application to the dodecane low-NO_x system. *Atmos. Chem. Phys.* **2012**, *12* (24), 11795−11817.

(98) Fortenberry, C. F.; Walker, M. J.; Zhang, Y.; Mitroo, D.; Brune, W. H.; Williams, B. J. Bulk and molecular-level characterization of laboratory-aged biomass burning organic aerosol from oak leaf and heartwood fuels. *Atmos. Chem. Phys.* **2018**, *18* (3), 2199−2224.

(99) Arthur Stankiewicz, B.; van Bergen, P. F.; Duncan, I. J.; Carter, J. F.; Briggs, D. E. G.; Evershed, R. P. Recognition of Chitin and Proteins in Invertebrate Cuticles Using Analytical Pyrolysis/Gas Chromatography and Pyrolysis/Gas Chromatography/Mass Spectrometry. *Rapid Commun. Mass Spectrom.* **1996**, *10* (14), 1747−1757.

(100) Fischer, M.; Scholz-Böttcher, B. M. Simultaneous Trace Identification and Quantification of Common Types of Microplastics in Environmental Samples by Pyrolysis-Gas Chromatography−Mass Spectrometry. *Environ. Sci. Technol.* **2017**, *51* (9), 5052−5060.

(101) Joseph, S. M.; Krishnamoorthy, S.; Paranthaman, R.; Moses, J. A.; Anandharamakrishnan, C. A review on source-specific chemistry, functionality, and applications of chitin and chitosan. *Carbohydrate Polymer Technologies and Applications* **2021**, *2*, No. 100036.

(102) Vermeuel, M. P.; Millet, D. B.; Farmer, D. K.; Pothier, M. A.; Link, M. F.; Riches, M.; Williams, S.; Garofalo, L. A. Closing the Reactive Carbon Flux Budget: Observations From Dual Mass Spectrometers Over a Coniferous Forest. *J. Geophys. Res.: Atmos.* **2023**, *128* (14), e2023JD038753.

(103) Yazdani, A.; Dudani, N.; Takahama, S.; Bertrand, A.; Prévôt, A. S. H.; El Haddad, I.; Dillner, A. M. Characterization of primary and aged wood burning and coal combustion organic aerosols in an environmental chamber and its implications for atmospheric aerosols. *Atmos. Chem. Phys.* **2021**, *21* (13), 10273−10293.

(104) Hendrickson, E.; Minor, E. C.; Schreiner, K. Microplastic Abundance and Composition in Western Lake Superior As Determined via Microscopy, Pyr-GC/MS, and FTIR. *Environ. Sci. Technol.* **2018**, *52* (4), 1787−1796.